A right-invariant Riemannian distance on $\mathrm{GL}^+(n)$ and hypothesis testing on Jacobian matrices.

Ernesto Zacur, Matias Bossa, and Salvador Olmos, for the Alzheimer's Disease Neuroimaging Initiative**

GTC, I3A, Universidad de Zaragoza
Maria de Luna 1, 50018 Zaragoza, Spain
{zacur,bossa,olmos}@unizar.es

Abstract. Tensor-based morphometry (TBM) studies encode the anatomical information in spatial deformations, which are locally characterized by Jacobian matrices. Current methods perform statistical analysis on incomplete features of the Jacobian matrices, such as their determinants or the Cauchy-Green deformation tensor. In this work we propose the use of a right-invariant Riemannian distance on $\mathrm{GL}^+(n)$, providing more information about the local deformation than previous approaches.

1 Introduction

Tensor-based morphometry (TBM) is a methodology to analyze anatomical information encoded by the spatial transformations that map a reference template to a set of images. The spatial mappings are estimated by means of non-rigid registration. Afterwards, voxel-wise statistical analysis is performed on the spatial derivatives of the deformations (Jacobian matrices, hereinafter denoted by $\mathbf{J}(\mathbf{x})$ for each location $\mathbf{x}$ of the template domain).

The simplest and still most widely used approach for TBM is based on the Jacobian determinant. This feature has two main advantages. Firstly, it has an intuitive interpretation because it represents the local volume change. Secondly, standard univariate statistical analysis can be easily performed on Jacobian determinants (or their logarithms) [1, 2]. The main limitation of the Jacobian determinant is that it only provides a coarse description of the deformation, because it only quantifies local volume change. To overcome this limitation, a multivariate TBM has been proposed based on the Cauchy-Green deformation tensor, $\mathbf{C} = \mathbf{J}^T\mathbf{J}$ which provides more complete description of the local deformation.

Most of the available statistical tools are well defined for Euclidean data. However, so far there are no many statistical tools for manifold-valued data,

** Data used in preparation of this article were obtained from the Alzheimer's Disease Neuroimaging Initiative (ADNI) database (adni.loni.ucla.edu). As such, the investigators within the ADNI contributed to the design and implementation of ADNI and/or provided data but did not participate in analysis or writing of this report. A complete listing of ADNI investigators can be found at: http://adni.loni.ucla.edu/wp-content/uploads/how_to_apply/ADNI_Acknowledgement_List.pdf

such as Cauchy-Green deformation tensors or Jacobian matrices. Statistics on Lie groups were analyzed in [3, 4] defining principal geodesic analysis. Analysis of diffusion tensor images (DTI) promoted the development of statistical tools on symmetric positive definite (SPD) tensors [5–8]. Some recent works deal with principal geodesics analysis using both, intrinsic statistics and the tangent plane approximation [9] and regression on manifold data [10–12]. A multivariate extension of the Hotelling's T^2 test has been proposed for analyzing longitudinal data [13].

In these previous works the definition of an appropriate distance between manifold elements plays an important role. The statistical tools for TBM studies use Jacobian matrices as input data which belong to the general linear group $\mathrm{GL}^+(n)$. A contribution of this work is the use of distances between Jacobian matrices for TBM studies. A further requirement for a TBM study is that statistical results should be independent of the template choice. Under a transitive non-rigid registration process, we will show that the use of right-invariant distances provides a sufficient condition for holding the template invariance requirement.

The aim of this paper is twofold. Firstly, to introduce a distance between Jacobian matrices for TBM studies. This is formulated as a right-invariant Riemannian distance on $\mathrm{GL}^+(n)$. The second aim is to illustrate results on a synthetic spatial deformation study and a MRI brain image study using three different right-invariant distances: d_{DET} which is a distance based on Jacobian determinants; d_{AFF} which is based on Cauchy-Green deformation tensors; and d_{RI} which is a Riemannian metric on $\mathrm{GL}^+(n)$. Voxel-wise hypothesis testing is performed by means of the Cramér test [14, 15] for several reasons: it is computed from the set of distances between observations solely and it can be used for both univariate and multivariate data.

2 Background on univariate/multivariate TBM

Let $\boldsymbol{\Phi} = [\phi^1, \phi^2, \cdots, \phi^n]^T \colon \Omega \to \Upsilon$ be an invertible, orientation preserving and differentiable spatial mapping (a diffeomorphism), where Ω and Υ are simply connected subsets of $\mathbb{R}^n$. Up to first order $\boldsymbol{\Phi}(\mathbf{x}+\mathrm{d}\mathbf{x}) = \boldsymbol{\Phi}(\mathbf{x}) + \mathbf{J}(\mathbf{x})\mathrm{d}\mathbf{x} + O(\mathrm{d}\mathbf{x}^2)$, where $\mathbf{J}$ is a field of linear transformations belonging to $\mathrm{GL}^+(n)$ ($\mathbf{J} \colon \Omega \to \mathrm{GL}^+(n)$). Every element $\mathbf{J}(\mathbf{x})$ is an $n \times n$ matrix with positive determinant. The set of these matrices together with the matrix-matrix multiplication is a matrix group and therefore a Lie group [16]. The n^2 elements of the matrix $\mathbf{J}(\mathbf{x}) = (\mathcal{D}\boldsymbol{\Phi})\big|_{\mathbf{x}}$ are the spatial derivatives of the deformation, such that the element $\mathbf{J}^{i,j}(\mathbf{x}) = \partial_j \phi^i\big|_{\mathbf{x}}$, *i.e.* the derivative of the i-th component of $\boldsymbol{\Phi}$ along the j-th coordinate.

Let T and A be two images representing similar contents. Registration of T and A is formulated as finding the spatial transformation $\boldsymbol{\Phi} \colon \mathrm{dom}(\mathsf{T}) \to \mathrm{dom}(\mathsf{A})$ such that $\boldsymbol{\Phi} \star \mathsf{T} \sim \mathsf{A}$, where $\star$ denotes the action on the image $(\boldsymbol{\Phi} \star \mathsf{T})(\mathbf{x}) = \mathsf{T}(\boldsymbol{\Phi}^{-1}(\mathbf{x}))$, and $(\cdot \sim \cdot)$ refers to an equivalence relation defined typically by a matching energy. Once the matching is found, both, the target image A and the

deformed image $\boldsymbol{\Phi} \star \mathsf{T}$ look spatially similar and a correspondence is obtained between all points of the domains dom(T) and dom(A).

In order to asses statistical differences between two groups of images $\mathcal{A} = \{\mathsf{A}_a\}$ and $\mathcal{B} = \{\mathsf{A}_b\}$ at each location a hypothesis test is performed on the corresponding Jacobian matrices. Just to fix notation, let $\boldsymbol{\Phi}_\mu$ be the mapping registering the template T to the image A_μ such that $\boldsymbol{\Phi}_\mu \star \mathsf{T} \sim \mathsf{A}_\mu$, and let $\mathbf{J}_\mu(\mathbf{x})$ be its corresponding Jacobian matrix at the point $\mathbf{x} \in \text{dom}(\mathsf{T})$. From now on, the subindexes a or a' run over the elements of the set $\mathcal{A}$, b or b' runs over the set $\mathcal{B}$, and, in general, indexes μ and ν run over any instance.

In order to perform statistics on Jacobian matrices an appropiate distance function $d(\cdot,\cdot)\colon \text{GL}^+(n) \times \text{GL}^+(n) \to \mathbb{R}^+$ must be employed.

2.1 Invariance with respect to the template

The template define the anatomical coordinates where to perform the statistical analysis. It is desired and expected that the methodology provides mainly the same result for any template choice allowing to make general statements about the anatomical location of the findings. Let T and W be two possible templates. Let $\boldsymbol{\Psi}$ be the mapping relating W and T such that, $\boldsymbol{\Psi} \star \mathsf{W} \sim \mathsf{T}$. Every point $\mathbf{y} \in \text{dom}(\mathsf{W})$ is in correspondence with a point $\mathbf{x} = \boldsymbol{\Psi}(\mathbf{y}) \in \text{dom}(\mathsf{T})$. Let $\tilde{\boldsymbol{\Phi}}_\mu$ be the spatial deformation to register W to A_μ. In this work it is assumed that the registration process is transitive [17, 18] and therefore $\tilde{\boldsymbol{\Phi}}_\mu = \boldsymbol{\Phi}_\mu \circ \boldsymbol{\Psi}$. Although this assumption is rarely achieved by current registration methods it is a key ingredient to describe the findings in anatomical coordinates irrespectively of the selected template.

The Jacobian matrix field derived from $\tilde{\boldsymbol{\Phi}}_\mu$ is given by $\tilde{\mathbf{J}}_\mu(\mathbf{y}) = \mathbf{J}_\mu(\boldsymbol{\Psi}(\mathbf{y}))\mathbf{P}(\mathbf{y})$, where $\mathbf{P}(\mathbf{y}) = (\mathcal{D}\boldsymbol{\Psi})\big|_{\mathbf{y}}$. For a statistic based on distances, a sufficient condition to achieve template invariance is to use a distance which fulfills

$$d(\tilde{\mathbf{J}}_\mu(\mathbf{y}), \tilde{\mathbf{J}}_\nu(\mathbf{y})) = d(\mathbf{J}_\mu(\mathbf{x})\mathbf{P}(\mathbf{y}), \mathbf{J}_\nu(\mathbf{x})\mathbf{P}(\mathbf{y})) = d(\mathbf{J}_\mu(\mathbf{x}), \mathbf{J}_\nu(\mathbf{x}))$$

which is accomplished by a right-invariant distance, *i.e.*

$$d(\mathbf{J}_\mu\mathbf{P}, \mathbf{J}_\nu\mathbf{P}) = d(\mathbf{J}_\mu, \mathbf{J}_\nu) \tag{1}$$

for any $\mathbf{J}_\mu, \mathbf{J}_\nu, \mathbf{P} \in \text{GL}^+(n)$.

2.2 Jacobian determinant

The most widely used tests to assess group differences are based on the determinant of Jacobian matrices. These determinants belong to the group of positive numbers under multiplication. This is a Lie group and an invariant distance is

$$d_{DET}(\mathbf{J}_\mu, \mathbf{J}_\nu) = |\log(\det(\mathbf{J}_\mu)) - \log(\det(\mathbf{J}_\nu))|\,. \tag{2}$$

The determinant of a Jacobian matrix can only quantify local volume changes. Note that d_{DET} does not satisfy the coincidence axiom which can be seen by the fact that $d_{DET}(\mathbf{J}, \mathbf{LJ}) = d_{DET}(\mathbf{J}, \mathbf{JL}) = 0$ for any matrix $\mathbf{L}$ with $\det(\mathbf{L}) = 1$.

2.3 Deformation tensor

In the area of continuum mechanics a commonly used feature to measure a local deformation at the point $\mathbf{x}$ is the called Cauchy-Green deformation tensor [19] $\mathbf{C}(\mathbf{x}) = \mathbf{J}^T(\mathbf{x})\mathbf{J}(\mathbf{x})$. The tensor $\mathbf{C}$ is a symmetric positive definite (SPD) matrix and it is related to the amount of anisotropic deformation up to a rotation. Under a change of template, Jacobian matrices transform as $\mathbf{J} \mapsto \mathbf{JP}$ and therefore Cauchy-Green deformation tensors transform as $\mathbf{C} \mapsto \mathbf{P}^T\mathbf{CP}$.

In [5, 6] a distance between SPD matrices was proposed[1]: $d_{SPD}(\mathbf{C}_\mu, \mathbf{C}_\nu) = \left\| \operatorname{logm}\left((\mathbf{C}_\mu)^{-1/2}(\mathbf{C}_\nu)(\mathbf{C}_\mu)^{-1/2}\right)\right\|_F$ and for for any $\mathbf{P}$ with positive determinant satisfies $d_{SPD}(\mathbf{C}_\mu, \mathbf{C}_\nu) = d_{SPD}(\mathbf{P}^T\mathbf{C}_\mu\mathbf{P}, \mathbf{P}^T\mathbf{C}_\nu\mathbf{P})$. The distance d_{SPD} defines a distance between Jacobian matrices

$$d_{AFF}(\mathbf{J}_\mu, \mathbf{J}_\nu) = \left\| \operatorname{logm}\left((\mathbf{J}_\mu^T\mathbf{J}_\mu)^{-1/2}(\mathbf{J}_\nu^T\mathbf{J}_\nu)(\mathbf{J}_\mu^T\mathbf{J}_\mu)^{-1/2}\right)\right\|_F \tag{3}$$

satisfying $d_{AFF}(\mathbf{J}_\mu, \mathbf{J}_\nu) = d_{AFF}(\mathbf{J}_\mu\mathbf{P}, \mathbf{J}_\nu\mathbf{P})$ and therefore fulfills the template invariance requirement.

Likewise d_{DET}, the distance d_{AFF} does not satisfy the coincidence axiom, specifically $d_{AFF}(\mathbf{J}, \mathbf{RJ}) = 0$ for any rotation $\mathbf{R}$.

3 A metric on $\mathbf{GL}^+(n)$

The two previous distances fulfill the template invariance requirement. However they do not satisfy the coincidence axiom and accordingly some differences may not be measured. To overcome this drawback a right-invariant Riemannian metric on the space of Jacobian matrices is presented below.

3.1 Invariant Riemannian distances on Lie groups

Let $\mathcal{M}$ be a differentiable manifold and $T_z\mathcal{M}$ its tangent space at the element $z \in \mathcal{M}$. A Riemannian metric $(\mathcal{M}, \langle u, v\rangle_z)$ on $\mathcal{M}$ is a smooth assignment of inner products to every tangent space where $z \in \mathcal{M}$ and $u, v \in T_z\mathcal{M}$ [20]. Using this assignment, the length of a curve segment $\gamma : [t_0, t_1] \subset \mathbb{R} \to \mathcal{M}$ is defined as

$$\operatorname{Length}(\gamma; t_0, t_1) = \int_{t_0}^{t_1} \langle \dot\gamma_{(s)}, \dot\gamma_{(s)}\rangle_{\gamma(s)}^{1/2} \mathrm{d}s\,.$$

A geodesic segment between two elements z and w belonging to $\mathcal{M}$ is an arc-length parameterized curve segment which locally minimizes the length. The Riemannian distance between z and w is the length of the shortest geodesic segment connecting both elements.

Geodesics can be uniquely described by an initial point and an initial velocity. This description is related to the Riemannian exponential function $\operatorname{Exp}_z(v)$

[1] $\operatorname{logm}(\cdot)$ denotes the matrix logarithm (the inverse of the matrix exponential, denoted as $\operatorname{expm}(\cdot)$) and $\|\cdot\|_F$ is the Frobenius norm.

where $v \in T_z\mathcal{M}$ [21]. The curve generated by $\mathrm{Exp}_z(tv)$ is a geodesic and the length of the segment from $t = 0$ to $t = 1$ is equal to $\langle v, v\rangle_z^{1/2}$.

The set $\mathrm{GL}^+(n)$ of all $n \times n$ matrices with positive determinant can be endowed with a differentiable manifold structure [16]. Furthermore, it has a Lie group structure (defined by the matrix-matrix product) and their elements, curves, tangent spaces and velocities can be translated by its group action [22].

A right-invariant metric is a Riemannian metric which naturally arises in Lie groups. Under this metric geodesics and distances remain invariant under right-translations. The metric can be defined as an inner product at a single tangent space (usually at $T_I\mathcal{M}$, called the group algebra) and propagated from right to the whole group

$$\langle u, v\rangle_z = \langle T_z\boldsymbol{R}_y u, T_z\boldsymbol{R}_y v\rangle_{zy}\,,$$

where $T_z\boldsymbol{R}_y$ is the tangent lift of the $\boldsymbol{R}_y$ operator and right-translates a velocity from $T_z\mathcal{M}$ to $T_{zy}\mathcal{M}$. Additionally the following invariance property of the Riemannian exponential function holds:

$$\mathrm{Exp}_z(v) = \mathrm{Exp}_I(T_z\boldsymbol{R}_{z^{-1}}v)z\,. \tag{4}$$

For a matrix group the tangent lift of the right translation takes the form $T\boldsymbol{R}_z v \mapsto \mathbf{VZ}$, where $\mathbf{V}$ and $\mathbf{Z}$ are a matrix representation of v and z.

3.2 Riemannian right-invariant distance on $\mathrm{GL}^+(n)$

A closed form solution for the invariant Riemannian exponential on $\mathrm{GL}^+(n)$ for the case where $\langle \mathbf{U}_1, \mathbf{U}_2\rangle_{\mathbf{I}} = \mathrm{trace}(\mathbf{U}_1^T\mathbf{U}_2)$, being $\mathbf{U}_1$ and $\mathbf{U}_2$ elements of $T_{\mathbf{I}}\mathrm{GL}^+(n)$, was given in[2] [23]:

$$\begin{aligned}\mathrm{Exp}_{\mathbf{Q}}(\mathbf{V}) &= \mathrm{Exp}_{\mathbf{I}}(\mathbf{U})\mathbf{Q} \\ &= \mathrm{expm}\left(\mathbf{U} - \mathbf{U}^T\right)\mathrm{expm}\left(\mathbf{U}^T\right)\mathbf{Q}\,,\end{aligned} \tag{5}$$

where $\mathbf{V} \in T_{\mathbf{Q}}\mathrm{GL}^+(n)$ and $\mathbf{U} = \mathbf{VQ}^{-1} \in T_{\mathbf{I}}\mathrm{GL}^+(n)$.

From the right-invariant Riemannian metric on $\mathrm{GL}^+(n)$ the following distance is induced:

$$d_{RI}(\mathbf{J}_\mu, \mathbf{J}_\nu) = \langle \mathbf{U}^*, \mathbf{U}^*\rangle_{\mathbf{J}_\mu}^{1/2}\,,$$

where $\mathbf{U}^*$ is the smallest initial velocity satisfying $\mathrm{Exp}_{\mathbf{I}}(\mathbf{U})\mathbf{J}_\mu = \mathbf{J}_\nu$. The distance inherits the right-invariance from the metric, $d_{RI}(\mathbf{J}_\mu, \mathbf{J}_\nu) = d_{RI}(\mathbf{J}_\mu\mathbf{P}, \mathbf{J}_\nu\mathbf{P})$ for any $\mathbf{P}$ in $\mathrm{GL}^+(n)$, and therefore the invariance under the template holds. In addition, d_{RI} fulfills the coincidence axiom, *i.e.* $d_{RI}(\mathbf{J}_\mu, \mathbf{J}_\nu) = 0$ if and only if $\mathbf{J}_\mu = \mathbf{J}_\nu$.

[2] Actually, in [23] the closed-form solution is given for a left-invariant Riemannian metric, however using the identity $\mathrm{Exp}_{\mathbf{I}}^{right}(\mathbf{U}) = (\mathrm{Exp}_{\mathbf{I}}^{left}(-\mathbf{U}))^{-1}$ it is possible to express in closed-form its right-invariant version.

In this work it is proposed to compute the Riemannian distance solving the following problem:

$$\underset{\mathbf{U}\in T_{\mathbf{I}}\mathrm{GL}^+(n)}{\text{minimize}} \quad \left\|\mathrm{Exp}_{\mathbf{I}}(\mathbf{U})\mathbf{J}_\mu - \mathbf{J}_\nu\right\|_F^2 \quad , \tag{L1}$$

where, for simplicity, the Frobenius norm was chosen.

The Riemannian exponential function under a right-invariant metric is a surjective mapping to the identity component of the group. As the group $\mathrm{GL}^+(n)$ consists of only one connected component, then the distance is well defined for any pair of elements.

Using the right-invariance property in eq. (4), it is possible to reformulate the problem (L1) as

$$\underset{\mathbf{U}\in\mathfrak{gl}(n)}{\text{minimize}} \quad \left\|\mathrm{Exp}_{\mathbf{I}}(\mathbf{U}) - \mathbf{J}_\nu\mathbf{J}_\mu^{-1}\right\|_F^2 \quad , \tag{L2}$$

where $\mathfrak{gl}(n) \equiv \mathbb{R}^{n\times n}$ is the Lie algebra of $\mathrm{GL}^+(n)$.

A gradient descent procedure can be used to solve (L2) where the gradient with respect to $\mathbf{U}$ is needed. Let $\mathbf{Q} \in \mathrm{GL}^+(n)$ and $E(\mathbf{U};\mathbf{Q}) = \left\|\mathrm{Exp}_{\mathbf{I}}(\mathbf{U}) - \mathbf{Q}\right\|_F^2 = \left\|\mathrm{expm}(\mathbf{U}-\mathbf{U}^T)\mathrm{expm}(\mathbf{U}^T) - \mathbf{Q}\right\|_F^2$ be the objective function. Its derivative with respect to $\mathbf{U}$ results in

$$\mathcal{D}_{\mathbf{U}}E(\mathbf{U};\mathbf{Q}) = 2\left(\overline{\mathrm{Exp}_{\mathbf{I}}(\mathbf{U})} - \overline{\mathbf{Q}}\right)^T \mathcal{D}_{\mathbf{U}}\mathrm{Exp}_{\mathbf{I}}(\mathbf{U})\,, \tag{6}$$

where $\overline{\mathbf{M}}$ denotes the n^2 dimensional vector resulting by the stacking of the columns of $\mathbf{M}$. $\mathcal{D}$ is the Fréchet derivative operator: for a matrix function of matrix argument $\mathbf{F}\colon \mathbb{R}^{m\times n} \to \mathbb{R}^{p\times q}$, $\mathcal{D}_{\mathbf{M}}\mathbf{F}(\mathbf{M})$ is a $(pq)\times(mn)$ linear operator fulfilling $[\mathcal{D}_{\mathbf{M}}\mathbf{F}(\mathbf{M})]^{i,j} = \partial_{\overline{\mathbf{M}}^j}\overline{\mathbf{F}(\mathbf{M})}^i$. Some rules to compute matrix functions derivatives are in [24, Chapter 13].

Deriving the expression in eq. (5) it is obtained

$$\begin{aligned}\mathcal{D}_{\mathbf{U}}\mathrm{Exp}_{\mathbf{I}}(\mathbf{U}) = {} & \left(\mathbf{I}_n \otimes \mathrm{expm}(\mathbf{U}-\mathbf{U}^T)\right)\mathrm{dexpm}(\mathbf{U}^T)\mathbf{K}_{nn} + \\ & + \left(\mathrm{expm}(\mathbf{U})\otimes\mathbf{I}_n\right)\mathrm{dexpm}(\mathbf{U}-\mathbf{U}^T)\left(\mathbf{I}_{n^2} - \mathbf{K}_{nn}\right)\end{aligned} \tag{7}$$

where $\mathbf{I}_m$ is the $m\times m$ identity matrix, $\mathbf{K}_{nn}$ is the commutation matrix [24] defined by $\mathbf{K}_{nn}\overline{\mathbf{X}} = \overline{\mathbf{X}^T}$ for an $n\times n$ matrix $\mathbf{X}$ and $\mathrm{dexpm}(\cdot)$ is the Fréchet derivative of the matrix exponential function (see Appendix A).

The optimization problem to compute d_{RI} is presented as an iterative descent optimization with a backtracking line-search along the direction $-\mathcal{D}_{\mathbf{U}}E(\mathbf{U};\mathbf{Q})$ given by eq. (6).

Once the optimal initial velocity $\mathbf{U}^*$ is obtained, the length of the geodesic segment is $\langle\mathbf{U}^*,\mathbf{U}^*\rangle_{\mathbf{I}}^{1/2} = \left\|\mathbf{U}^*\right\|_F$. If its Riemannian exponentiation generate the shortest curve segment between $\mathbf{I}$ and $\mathbf{J}_\nu\mathbf{J}_\mu^{-1}$, then $d_{RI}(\mathbf{J}_\mu,\mathbf{J}_\nu) = d_{RI}(\mathbf{I},\mathbf{J}_\nu\mathbf{J}_\mu^{-1}) = \left\|\mathbf{U}\right\|_F$.

While the existence of a zero minimizer is guaranteed, a drawback of this formulation is the non-uniqueness of a velocity satisfying $\mathrm{Exp}_{\mathbf{I}}(\mathbf{U}) = \mathbf{Q}$. There may exist different initial velocities which generate geodesics segments between $\mathbf{J}_\mu$ and $\mathbf{J}_\nu$.

4 Cramér test

Three different distance functions over Jacobian matrices have been considered in previous sections: d_{DET}, d_{AFF} and d_{RI}. Even though many statistical analysis tools can be defined from the set of distances among observations, this work focused on the Cramér two-sample test [14, 15]. This test was selected because its statistic depends only on the inter-point distances

$$\sigma(\{D_{\mu\nu}\}) = \frac{n_a n_b}{n_a + n_b}\left(\frac{1}{n_a n_b}\sum_{a=1}^{n_a}\sum_{b=1}^{n_b} D_{ab} - \frac{1}{2n_a^2}\sum_{a=1}^{n_a}\sum_{a'=1}^{n_a} D_{aa'} - \frac{1}{2n_b^2}\sum_{b=1}^{n_b}\sum_{b'=1}^{n_b} D_{b'b}\right)$$

where $D_{\mu\nu} = d(\mathbf{J}_\mu, \mathbf{J}_\nu)$ is the inter-element distance and n_a and n_b is the cardinality of the set $\mathcal{A}$ and $\mathcal{B}$ respectively. Accordingly, this test can be directly used on both univariate and multivariate data.

Statistical significance can be assessed by means of random permutation tests. The distribution of the statistic under the null hypothesis is empirically estimated from random permutations of the group labels. The null hypothesis is that both groups instances are drawn from the same distribution and it is rejected for large enough values of σ. The p-value is assessed as the proportion of the permutations having a σ value larger or equal than the σ value without relabeling.

In TBM studies hypothesis tests are assessed at each image location and therefore multiple comparison correction is an important issue. In this work the *false discovery rate* (FDR) [25] criterion was used for the correction of the proportion of false-positives among the rejected null hypotheses.

5 Results

5.1 Synthetic study

A synthetic study was designed to generate a set of controlled deformations which will allow to illustrate the results of the three right-invariant distances in a TBM application environment.

In order to facilitate the visualization of the results the experiment was performed generating deformations on a 2D image. Two sets of 50 deformation fields were generated to deform a template. The first set was designed to represent the anatomical variability within a 'control' group, while the second set aimed at representing a 'pathological' group with group-driven anatomical differences and intra-group variability. Representative examples of the deformation maps

are illustrated in Fig. 1. Fig. 1 also shows 5 deformed contours from 'control' and 'pathological' groups depicting the intra-group variabilities.

Deformation instances for 'control' group $\mathcal{A}$ were modeled as smooth and invertible random deformation fields which were obtained by integration of a spatially correlated stationary velocity field. Instances for 'pathological' group $\mathcal{B}$ were modeled as the composition of a common group-driven deformation and random deformations similar to ones used for the 'control' group. The group-driven deformation was designed as an invertible mapping producing the following changes on the 'subcortical structures': a clockwise rotation of the structure in the 'left hemisphere' of 15 degrees; a counter-clockwise rotation of the structure in the 'right hemisphere' of 15 degrees and a subsequent anisotropical scaling with factors 0.7 and $1/0.7$ along the horizontal and vertical directions respectively. Note that the group-driven deformation preserves the volume of the 'subcortical structures' but the surrounding regions suffer more complex deformation due to the continuity of the deformations. This effect can be seen in the zoomed panel of Fig. 1.

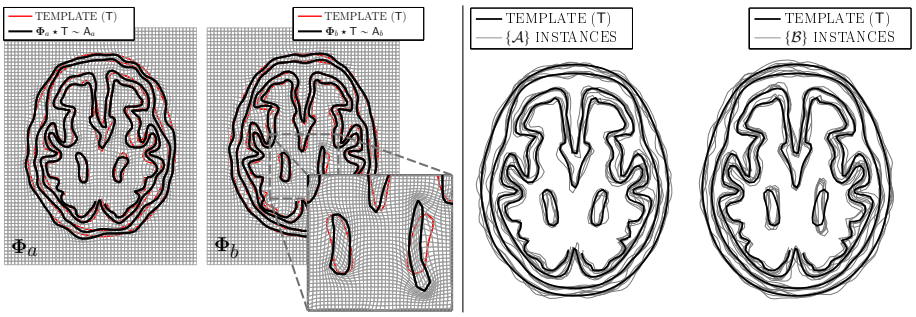

Fig. 1. Synthetic data for 'control' group and 'pathological' group. Left: illustrative examples of the deformations map $\boldsymbol{\Phi}_a$ and $\boldsymbol{\Phi}_b$ mapping the template to a given instance. Right: five contours depicting the intra-group anatomical variability.

TBM studies were performed using the previous defined distances: d_{DET}, d_{AFF} and d_{RI}. At each location Cramér tests were computed and a set of 100,000 random permutations were performed in order to assess the p-value maps. In order to correct for multiple comparison, FDR criterion was used.

Fig. 2 shows the FDR corrected p-value maps corresponding to the Cramér tests. The distance d_{DET} was not able to detect statistically significant volume changes in the interior of the 'subcortical structures', because there was no significant local volume changes in those regions. However, significant volume differences were found at outer regions surrounding these structures. This behavior shows that the deformations driven by a rotation of a structure surrounded by a static region mainly generates volume changes outside the structure.

The statistical map using d_{AFF} shows significant differences in the interior of the 'right subcortical structure', because there was an anisotropic scaling. However, no significant differences were found in the interior of the 'left subcortical structure' because the deformations were mainly driven by a rotation.

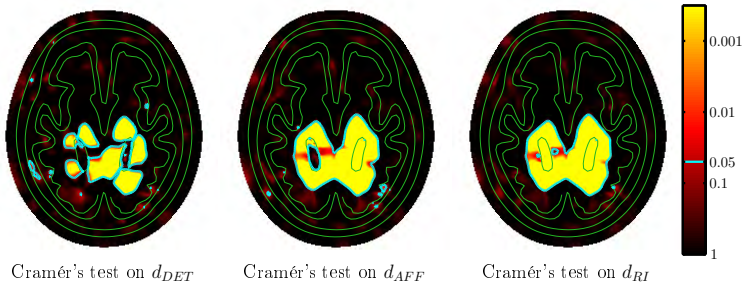

Fig. 2. Statistical map of FDR corrected p-values for Cramér test based on different distances. Template contours are illustrated in green for localization purposes. Cyan contours show the boundary of the regions with significant differences with the criterion of $p_{FDR} \leqslant 0.05$.

Regarding the statistical map using d_{RI}, it can be seen that significant differences were found in the interior of both 'subcortical structures'.

5.2 ADNI dataset

A set of T1-MRI brain images was selected from ADNI database (adni.loni.ucla.edu). Twenty elderly control subjects (denoted here as NOR group) and twenty AD patients (denoted as AD group) were selected from the database. As the brain atrophy is affected by factors such as age and gender, subjects were selected to be gender-matched and within a narrow age interval (72 ± 1 years). Clinical scores, such as MiniMental State Examination (MMSE) [26] or the memory score in the Clinical Dementia Ratio (CDR) [27], were significantly different between both groups under a Student's t-test (MMSE: 29.3 ± 1.0 for NOR group while 23.3 ± 1.8 for AD group; CDR: 0.0 ± 0.0 for NOR group while 0.9 ± 0.3 for AD group).

The MRI template T was built from 40 elderly control subjects as described in [2]. The deformations fields $\boldsymbol{\Phi}_\mu$ were estimated using a SVF diffeomorphic registration [28, 2] between the MRI template T and each image instance.

Voxel-wise Cramér tests were performed using the three right-invariant distances d_{DET}, d_{AFF} and d_{RI}. Critical values were estimated by means of a permutation test using 100,000 permutations. After, the p-values maps were corrected with FDR criterion. Fig. 3 shows a coronal and sagittal illustrative slice of the corrected p-value map for each method.

The three statistical maps are in agreement with the pathophysiological knowledge of Alzheimer's disease. As it was expected, the number of voxels with significant differences in the d_{DET} map was much smaller than in d_{AFF} and d_{RI} maps.

6 Conclusion

Previous literature on TBM focused on selecting different features or descriptors of the Jacobian matrix on which to perform either univariate or multivariate

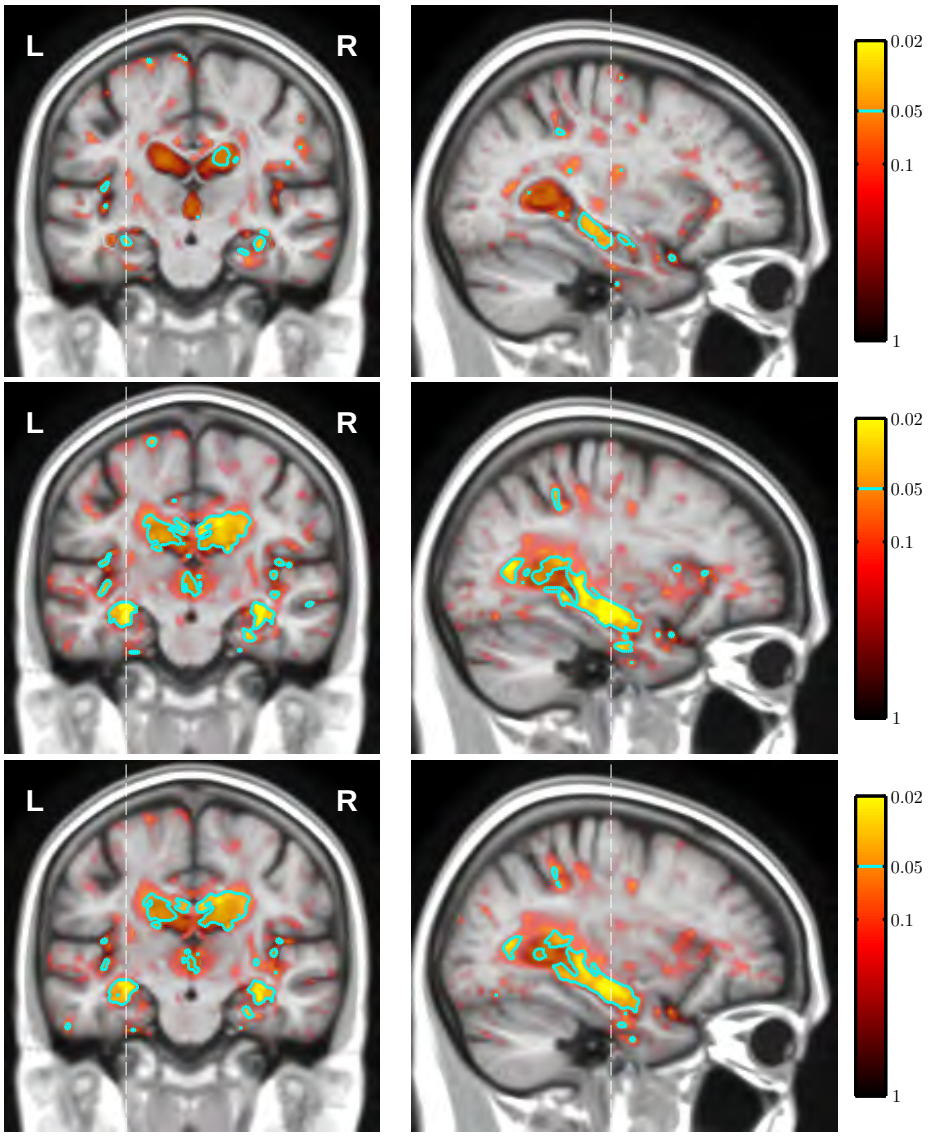

Fig. 3. Illustrative coronal (left) and sagittal (right) view of FDR-corrected p-value maps of the Cramér test on three right-invariant distances: d_{DET} (top row), d_{AFF} (middle row) and d_{RI} (bottom row). L and R denote left and right hemisphere respectively. The dashed vertical lines show the location of the sagittal and coronal slices.

statistics. In this work different distance functions over Jacobian matrices were analyzed. From this distance perspective, the template invariance requirement led to the use of right-invariant distances.

Three different right-invariant distances on $\mathrm{GL}^+(n)$ were considered in this work. The first two distances have been previously used in the literature: the distance between log of Jacobian determinants d_{DET} and a distance between

deformation tensors d_{AFF}. While the distance d_{DET} only measures local volume changes, d_{AFF} additionally quantifies anisotropic scalings and shearings but no local rotations. The third one is a right-invariant Riemannian distance between Jacobian matrices d_{RI}, and it has not been previously used on TBM. The Riemannian distance d_{RI} quantifies the complete local deformation. This behavior was clearly illustrated in the results from the synthetic data.

A Fréchet derivative of the matrix exponential

To compute the Fréchet derivative $\mathcal{D}_{\mathbf{U}}\mathrm{Exp}_{\mathbf{I}}(\mathbf{U})$ given in eq. (7) an expression for $\mathrm{dexpm}(\mathbf{M}) \equiv \mathcal{D}_{\mathbf{M}}\mathrm{expm}(\mathbf{M})$ is required. This is the linear operator containing the derivatives of each element of $\mathrm{expm}(\mathbf{M})$ with respect to a perturbation on each element of $\mathbf{M}$ and results in an $n^2 \times n^2$ matrix.

There are different attempts to compute $\mathcal{D}_{\mathbf{M}}\mathrm{expm}(\mathbf{M})$ [29–31]. For our computations we used the approach given in [32], where for an analytic matrix function $\mathbf{F}(\mathbf{M})$

$$\mathbf{F}\left(\left(\begin{array}{c|c}\mathbf{M} & \mathbf{P}\\ \hline \mathbf{0} & \mathbf{M}\end{array}\right)\right) = \left(\begin{array}{c|c}\mathbf{F}(\mathbf{M}) & \mathrm{d}_r\mathbf{F}(\mathbf{M}+r\mathbf{P})\\ \hline \mathbf{0} & \mathbf{F}(\mathbf{M})\end{array}\right)$$

and if $\mathbf{P}^j$ is the j-th canonical perturbation, then the vectorization of the upper-right submatrix $\overline{\mathrm{d}_r\mathbf{F}(\mathbf{M}+r\mathbf{P}^j)}$ is the j-th column of the matrix $\mathcal{D}_{\mathbf{M}}\mathbf{F}(\mathbf{M})$.

Acknowledgements

This work was funded by research grants TEC2009-14587-C03-01 from CICYT, AMIT project CEN-20101014 from CENIT program, CIM project IPT-2011-1638-900000 from INNPACTO program, Spain. Data collection and sharing for this project was funded by the Alzheimer's Disease Neuroimaging Initiative (ADNI) (National Institutes of Health Grant U01 AG024904).

References

1. Davatzikos, C., *et. al*: Voxel-based morphometry using the RAVENS maps: methods and validation using simulated longitudinal atrophy. NeuroImage **14**(6) (2001) 1361–1369
2. Bossa, M., Zacur, E., Olmos, S., ADNI: Tensor-based morphometry with stationary velocity field diffeomorphic registration: application to ADNI. NeuroImage **51**(3) (2010) 956–969
3. Fletcher, P.T.: Statistical Variability in Nonlinear Spaces: Application to Shape Analysis and DT-MRI. PhD thesis, University of North Carolina (2004)
4. Boisvert, J., *et. al*: Geometric variability of the scoliotic spine using statistics on articulated shape models. IEEE Trans. Med. Imaging **27**(4) (2008) 557–568
5. Moakher, M.: A differential geometric approach to the geometric mean of symmetric positive-definite matrices. SIAM J. Matrix Anal. Appl. **26**(3) (2005) 735–747
6. Batchelor, P.G., *et. al*: A rigorous framework for diffusion tensor calculus. Magn. Reson. Med. **53**(1) (2005) 221–225
7. Pennec, X., Fillard, P., Ayache, N.: A Riemannian framework for tensor computing. Int. J. Comput. Vis. **66**(1) (2006) 41–66
8. Fletcher, P.T., Joshi, S.: Riemannian geometry for the statistical analysis of diffusion tensor data. Signal Processing **87**(2) (2007) 250–262

9. Sommer, S., *et. al*: Manifold valued statistics, exact principal geodesic analysis and the effect of linear approximations. In: Europ. Conf. on Comp. Vision (2010) 43–56
10. Machado, L., Silva Leite, F., Krakowski, K.: Higher-order smoothing splines versus least squares problems on Riemannian manifolds. J. Dynam. Control Systems **16**(1) (2010) 121–148
11. Fletcher, P.T.: Geodesic regression on Riemannian manifolds. In: MFCA Workshop of MICCAI (2011) 86
12. Hinkle, J., *et. al*: Polynomial regression on Riemannian manifolds. arXiv preprint (2012)
13. Muralidharan, P., Fletcher, P.T.: Sasaki metrics for analysis of longitudinal data on manifolds. In: IEEE Conference on CVPR. (2012) 1027–1034
14. Baringhaus, L., Franz, C.: On a new multivariate two-sample test. J. Multivariate Anal. **88**(1) (2004) 190–206
15. Székely, G.J., Rizzo, M.L.: Testing for equal distributions in high dimension. InterStat **11**(5) (2004)
16. Tapp, K.: Matrix groups for undergraduates. AMS (2005)
17. Christensen, G.E., Johnson, H.J.: Invertibility and transitivity analysis for nonrigid image registration. Journal of Electronic Imaging **12**(1) (2003) 106–117
18. Škrinjar, O., Bistoquet, A., Tagare, H.: Symmetric and transitive registration of image sequences. Journal of Biomedical Imaging **2008** (2008) 14
19. Pennec, X.: Left-invariant Riemannian elasticity: a distance on shape diffeomorphisms? In: MFCA Workshop of MICCAI (2006) 1–13
20. Do Carmo, M.P.: Riemannian geometry. Birkhauser (1992)
21. Absil, P.A., Mahony, R., Sepulchre, R.: Optimization algorithms on matrix manifolds. Princeton Univ. Press (2009)
22. Hall, B.C.: Lie groups, Lie algebras, and representations: an elementary introduction. Springer (2003)
23. Andruchow, E., *et. al*: The left invariant metric in the general linear group. arXiv preprint (2011)
24. Abadir, K.M., Magnus, J.R.: Matrix algebra. Cambridge Univ. Press (2005)
25. Benjamini, Y., Hochberg, Y.: Controlling the false discovery rate: a practical and powerful approach to multiple testing. J. R. Stat Soc. Ser. B. **57** (1995) 289–300
26. Cockrell, J.R., Folstein, M.F.: Mini-mental state examination (MMSE). Psychopharmacol. Bull. **24**(4) (1988) 689–692
27. Morris, J.C.: The clinical dementia rating (CDR): current version and scoring rules. Neurology **43**(11) (Nov 1993) 2412–2414
28. Hernandez, M., Bossa, M., Olmos, S.: Registration of anatomical images using paths of diffeomorphisms parameterized with stationary vector field flows. Int. J. Comput. Vis. **85**(3) (2009) 291–306
29. Al-Mohy, A.H., Higham, N.J.: Computing the Fréchet derivative of the matrix exponential, with an application to condition number estimation. SIAM J. Matrix Anal. Appl. **30**(4) (2009) 1639–1657
30. Najfeld, I., Havel, T.F.: Derivatives of the matrix exponential and their computation. Adv. in Appl. Math. **16**(3) (1995) 321–375
31. Li, C., Sheng, Y., Wang, M.: An effective method to compute Fréchet derivative of matrix exponential and its error analysis. J. Inform. Comput. Sci. **7** (2010) 1854–1859
32. Mathias, R.: A chain rule for matrix functions and applications. SIAM J. Matrix Anal. Appl. **17**(3) (1996) 610–620